Vol 17 No 11, November 2008
1674-1056/2008/17(11)/4100-07

Chinese Physics B

© 2008 Chin. Phys. Soc.
and IOP Publishing Ltd

Numerical study of IP_3-induced Ca^{2+} spiral pattern evolution*

Tang Jun(唐 军)[a)b)†], Ma Jun(马 军)[b)c)], Yi Ming(易 鸣)[b)], and Jia Ya(贾 亚)[c)‡]

[a)] *College of Science, China University of Mining and Technology, Xuzhou* 221008, *China*
[b)] *Department of Physics and Institute of Biophysics, Huazhong Normal University, Wuhan* 430079, *China*
[c)] *Department of Physics, Lanzhou University of Technology, Lanzhou* 730050, *China*

(Received 19 May 2008; revised manuscript received 13 June 2008)

The effect of change in concentration of messenger molecule inositol 1,4,5-trisphosphate (IP_3) on intracellular Ca^{2+}spiral pattern evolution is studied numerically. The results indicate that when the IP_3 concentration decreases from 0.27 μM, a physiologically reasonable value, to different values, the spiral centre drifts to the edge of the medium and disappears for a small enough IP_3 concentration. The instability of spiral pattern can be understood in terms of excitability-change controlled by the IP_3 concentration. On the other hand, when the IP_3 concentration increases from 0.27 μM, a homogeneous area with a high Ca^{2+} concentration emerges and competes with the spiral pattern. A high enough IP_3 concentration can lead the homogeneous area to occupy the whole medium. The instability of spiral pattern is ascribed to the change in stability of a stationary state with a high Ca^{2+} concentration.

Keywords: spiral wave, Ca^{2+}, IP_3
PACC: 0545

As an interesting topic in pattern formations, spiral waves and their controls are often observed in a variety of excitable systems, such as Belousov–Zhabotinsky system,[1] the catalytic CO oxidation on Pt(110) surface,[2] the cAMP dynamics in Dictyostelium discoideum in the aggregation stage[3] and electrical activity in heart tissue.[4]

Intracellular Ca^{2+} is a primary regulator with varieties of cell functions, for example, early response to injury of brain tissue,[5] neurotransmitter release,[6] synaptic plasticity,[7] gene expression,[8] and cell death,[9] etc. Most of the Ca^{2+} that constitute the signal are released from intracellular stores, e.g. the endoplasmic reticulum (ER) or sarcoplasmic reticulum (SR), in which the normal Ca^{2+} concentration is very higher than that found intracellularly, into the intracellular space. This nonlinearly releasing process leads in many cells to the formation of spatiotemporal signals in the form of waves of high Ca^{2+} concentrations travelling across the cell. Intracellular calcium waves were first observed in medaka eggs[10] and later on in Xenopus oocytes,[11] etc. Intracellular Ca^{2+} spiral waves have often been observed in Xenopus oocytes[11−13] which here are seen as excitable media.

Many methods of controlling spirals are presented,[14−16] such as, external field, parameter perturbation, etc. As mentioned in Ref.[17], the degree of excitability in Xenopus oocytes is controlled by the IP_3 concentration. Furthermore, the IP_3 concentration is an experimentally controllable parameter, which can be stimulated and adjusted by binding extracellular agonists such as hormones or neurotransmitters to receptors in a membrane[18] or more accurately by photo-release of caged IP_3.[19] In this paper, Motivated by the importance to the excitability and experimental controllability of IP_3, we numerically study the effect of the IP_3 concentration on Ca^{2+} spiral pattern evolutions. The results show that when the IP_3 concentration decreases from 0.27 μM to different values, the spiral centre drifts to the edge of the medium and can disappear with a small enough variation in IP_3 concentration appearing. The instability of spiral can be understood in terms of excitability-change controlled by the IP_3 concentration. On the other hand, when the IP_3 concentration increases from 0.27 μM, a homogeneous area with a high Ca^{2+} concentration emerges and competes with the spiral pattern, and a large enough IP_3 concentration can lead the homogeneous area to occupy the whole medium. The instability of spiral pattern is ascribed

*Project supported by the National Natural Science Foundation of China (Grant Nos 10575041 and 10747005).
†E-mail: tjuns@phy.ccnu.edu.cn
‡E-mail: jiay@phy.ccnu.edu.cn

to the change in stability of a stationary state with high a Ca^{2+} concentration. We use a model involving mitochondrial Ca^{2+} uptake, which was developed first by Tang *et al*,[20] and modified to describe Ca^{2+} wave in Xenopus oocytes by Falcke *et al.*[17] The model is given by

$$\frac{\mathrm{d}c}{\mathrm{d}t} = v_{\mathrm{r}}(c_{\mathrm{r}} - c)\left[P_{\mathrm{r}}^{\mathrm{Leak}} + P_{\mathrm{r}}^{\mathrm{Chan}}\frac{c(1-n)}{c+\beta_1(1+K/I)}\right] - v_{\mathrm{m}}\left(V_{\max}^1\frac{c^2}{c^2+K_{\mathrm{d}}^2} - V_{\max}^2\frac{[\mathrm{Na}^+]^2}{[\mathrm{Na}^+]^2+K_{\mathrm{Na}}^2}\frac{m}{K_{\mathrm{m}}+m}\right) - v_{\mathrm{r}}P_{\mathrm{r}}^{\max}\frac{c^2}{c^2+K_{\mathrm{r}}^2} + D\nabla^2 c, \tag{1}$$

$$\frac{\mathrm{d}n}{\mathrm{d}t} = \varepsilon\left[\frac{c^2(1-n)}{\beta_2(c+\beta_1(1+K/I))} - n\right], \tag{2}$$

$$\frac{\mathrm{d}m}{\mathrm{d}t} = V_{\max}^1\frac{c^2}{c^2+K_{\mathrm{d}}^2} - V_{\max}^2\frac{[\mathrm{Na}^+]^2}{[\mathrm{Na}^+]^2+K_{\mathrm{Na}}^2}\frac{m}{K_{\mathrm{m}}+m}, \tag{3}$$

where c, c_{r}, and m denote the Ca^{2+} concentration in the cytosol, ER, and mitochondria, respectively. The fraction of inhibited ion channel is denoted by n. The ratio of the effective volume of the ER to the cytosolic volume is $v_{\mathrm{r}} = 0.185$, and the ratio of the effective volume of mitochondria to the cytosolic volume is $v_{\mathrm{m}} = 0.1$. Assume that no Ca^{2+} flux occurs across the cell membrane, the value of $C_{\mathrm{M}} = (c + v_{\mathrm{r}}c_{\mathrm{r}} + v_{\mathrm{m}}m)/(1 + v_{\mathrm{r}} + v_{\mathrm{m}})$ will be constant, which is set to be $1.56\,\mu$M. This allows c_{r} to be represented by $c_{\mathrm{r}} = [(1 + v_{\mathrm{r}} + v_{\mathrm{m}})C_{\mathrm{M}} - c - v_{\mathrm{m}}m]/v_{\mathrm{r}}$. $K = 0.8\,\mu$M is the effective dissociation constant for binding IP_3 to the ion channel.[21] I is the concentration of cytosolic IP_3 and the diffusive coefficient of Ca^{2+} D is $10\,\mu\mathrm{m}^2/\mathrm{s}$. The values of other parameters are $P_{\mathrm{r}}^{\mathrm{leak}} = 0.0097\,\mathrm{s}^{-1}$, $P_{\mathrm{r}}^{\mathrm{chan}} = 0.0097\mathrm{s}^{-1}$, $P_{\mathrm{r}}^{\max} = 5.31\,\mu$M/s, $\beta_1 = 0.12\,\mu$M, $\beta_2 = 0.1\,\mu$M, $\varepsilon = 0.15\,\mathrm{s}^{-1}$, $K_{\mathrm{r}} = 0.0296\,\mu$M, $K_{\mathrm{d}} = 1.5\,\mu$M, $K_{\mathrm{m}} = 1\,\mu$M, $V_{\max}^1 = 6.0\,\mu$M/s, $V_{\max}^2 = 3.0\,\mu$M/s, $[\mathrm{Na}^+] = 10\,\mathrm{mM}$, and $K_{\mathrm{Na}} = 5\,\mathrm{mM}$. The detailed meanings of these parameters may be found in Ref.[17].

The simulation is performed on a system of $500\,\mu\mathrm{m}\times500\,\mu\mathrm{m}$. The model Eqs.(1)–(3) are integrated using an Euler forward scheme, in spatial steps of $0.8\,\mu$m and time steps of $0.0005\,\mathrm{s}$.

Now we begin with $I = 0.27\,\mu$M which is a physiologically reasonable value for cytosolic IP_3 concentration. The local dynamics of this model can be understood in terms of the nullclines of the variables. In Fig.1, the nullclines of c and n are depicted by omitting the diffusive term in Eq.(1) and equating the terms on the right-hand sides of Eqs.(1)–(3) to 0. It can be seen that both nullclines intersect three times, thereby providing three fixed points. Thus the local dynamics of this model yields three stationary states. The stability analysis indicates that only the state with the lowest cytosolic Ca^{2+} concentration is stable and the cytosol behaves as an excitable system.

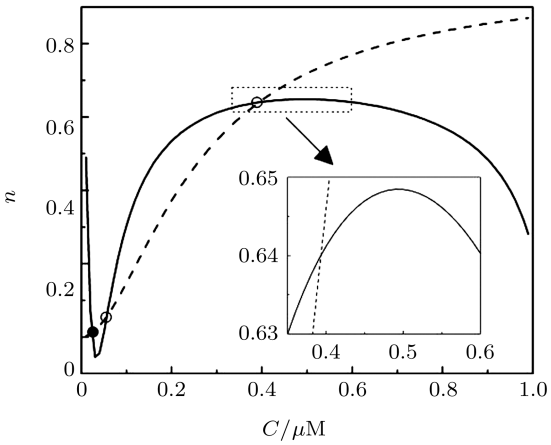


Fig.1. Nullclines of the Tang–Othmer model for $I = 0.27\,\mu$M. Solid line: c nullcline; Dashed line: n nullcline. Solid circle: stable fixed point; open circle: unstable fixed point. Inset: the amplified version of nullclines in the dashed rectangle.

Starting the system from a suitable initial condition, one can see that a spiral is fully developed at last (see Fig.2). The initial condition is that in a quadrate area, variable c decreases from left to right while n increases, and at positions out of the quadrate area, all variables c, n, and m are set as those in a rest state (see the left in Fig.2). The right in Fig.2 is a stable spiral picture at $t = 100\,\mathrm{s}$. In what follows, the IP_3 concentration will be changed from $I = 0.27\,\mu$M to different values. Thus the right in Fig.2 will be the picture at $t = 0\,\mathrm{s}$ for spiral pattern evolutions for different changed IP_3 concentrations.

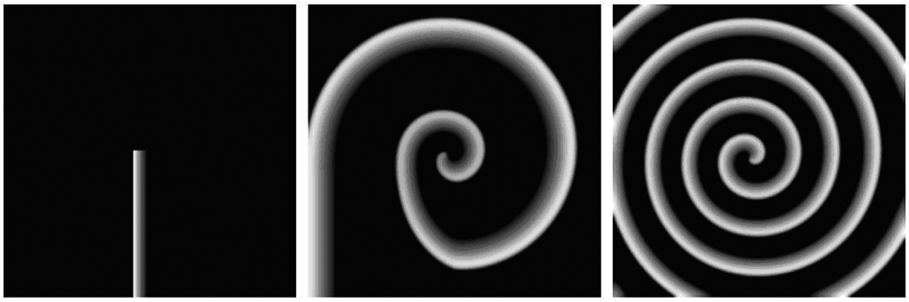


Fig.2. Time sequence illustrating the process of spiral developing from initial condition where $I = 0.27\,\mu$M. From left to right $t = 0$, 20, and 100 s. The black to white grey scale represents the lowest value 0 to the highest value 1 μM. This grey scale will be used in all figures in this paper.

Firstly, the IP_3 concentration is reduced to $0.1485\,\mu$M. Figure 3 shows the pattern evolution process, the central area of spiral gradually disappears, then the open end of remaining part will curl up into a new spiral tip which is far away from the central area. After enough time, new stable spiral pattern will be formed (see the right in Fig.3).



Fig.3. Time sequence illustrating the dynamics of spiral evolution when the IP_3 concentration is changed to 0.1485 μM at time $t = 0$ s. From left to right: $t = 10$, 20, and 200 s.

We have also simulated the pattern evolution processes for different changed IP_3 concentrations, and the results indicate that the tips of stable spiral drift away from the central area with the increase of the changed IP_3 concentration (see the top two parts in Fig.4). When the changed IP_3 concentration is small enough, not only the central area of spiral gradually disappears, but also the area far from the centre will be cut off into several parts, then several spiral tips will emerge (see the left bottom in Fig.4). Further the decreasing of the changed IP_3 concentration will cause the spiral tips to drift out of the medium (see the right bottom of Fig.4), then all spiral patterns totally disappear and the system stay in a stable stationary state with an extremely low Ca^{2+} concentration.

This kind of instability of spiral waves is ascribed to the decreasing of excitability due to a reduction in IP_3 concentration. Comparing with nullclines in Fig.1, with the decrease of IP_3 concentration, the two unstable stationary states tend to disappear, and the model will yield only one stationary state with a lowest Ca^{2+} concentration and the excitability decreases to a level which cannot maintain the stable spiral pattern. On the other hand, from a biological point of view, the decreasing of IP_3 concentration reduces the probability for Ca^{2+} to be released through ion channels because the binding of IP_3 to ion channels is a prerequisite for the activation of them. When the IP_3 concentration is low enough, extremely few Ca^{2+} ions can be released from ER through ion channels, i.e. the medium cannot be excited and no stable spiral pattern can be maintained.

Then the IP_3 concentration will be increased from $0.27\,\mu$M, and at each given changed IP_3 concentration, the pattern evolution process is simulated. From the

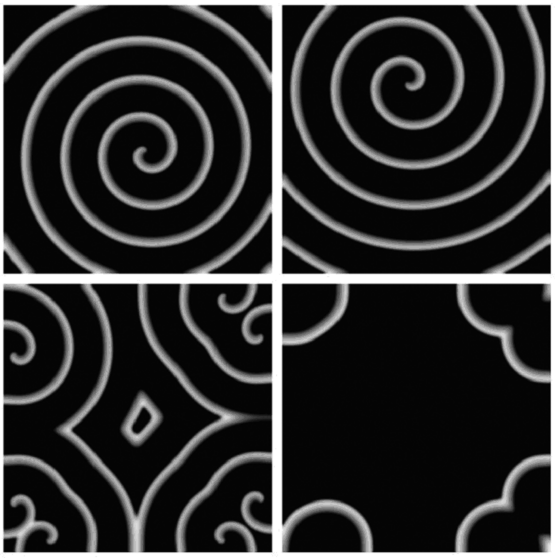


Fig.4. Well-developed spiral patterns after IP_3 concentration is changed to different values at time $t = 0$ s. From left to right and top to bottom, the changed IP_3 concentration $I = 0.1598$, 0.1493, 0.1480, and 0.1453 μM, and corresponding time $t = 120$, 120, 120, and 30 s, respectively.

simulation results, pattern-rich evolution behaviours are obtained. When IP_3 concentration is increased to a value less than 0.3133 μM, a stable spiral pattern can be maintained after a slight drift of spiral tip. In a very narrow region (0.3133–0.3183 μM) for a changed IP_3 concentration, the competition between two patterns is found (see Fig.5). If IP_3 concentration is changed to a value in the above-mentioned region, a homogeneous patch in a high Ca^{2+} concentration area appears in the spiral core, which gradually grows and pushes the spiral outward. But the homogeneous area with a high Ca^{2+} concentration cannot occupy the whole medium. After the homogeneous area has increased to about 75 percents of the whole medium, the remaining area, which has been compressed from a regular wave pattern to a turbulence-like pattern, in turn compress the homogeneous area. Finally the turbulence-like pattern occupies the whole medium. Then from the spatial points where the homogeneous area lastly disappears, some plane waves are emitted, and these plane waves collide with each other. As a result, the plane waves break and create open ends that finally curl up into spiral tips. To more clearly reveal the competition between two patterns, the Ca^{2+} concentration at the selected point (120 μm, 120 μm) is plotted against time in Fig.6. First, the selected point is regularly excited. After the selected point has been occupied by the homogeneous area, it is in a stable state. Then the point is regularly excited again after the point is reversely compressed out of the homogeneous area.

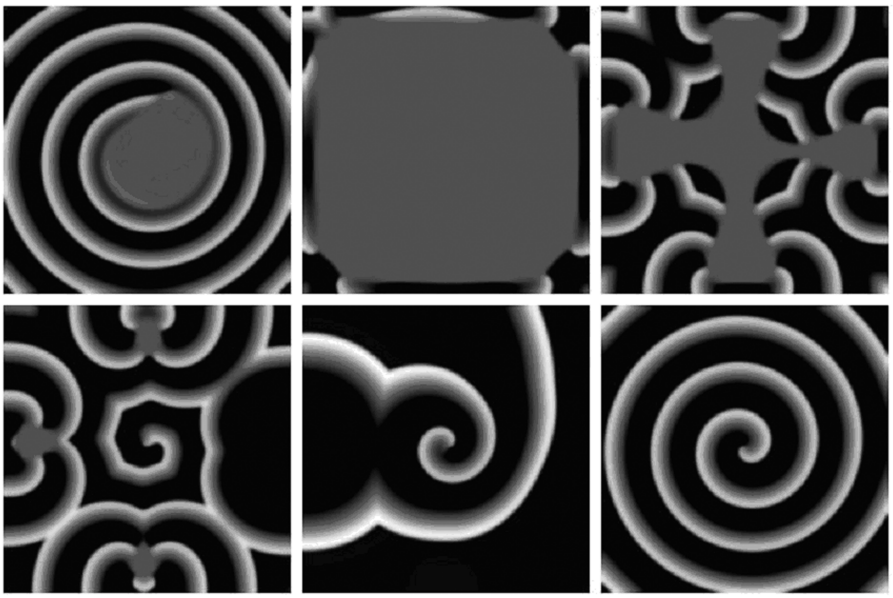


Fig.5. Time sequence illustrating the dynamics of spiral evolution when IP_3 concentration is changed to 0.3158 μM. From left to right and up to bottom, $t = 100$, 300, 530, 600, 680, and 750 s.

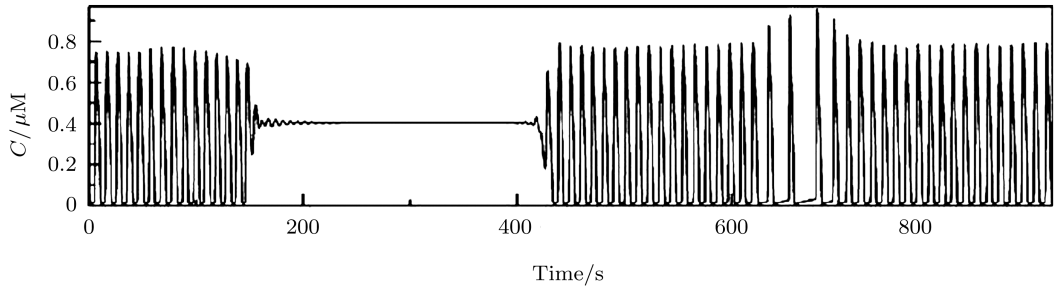


Fig.6. Time evolution of Ca^{2+} concentration at a point (120 μm, 120 μm).

We change the IP_3 concentration to a larger value. Figure 7 shows the pattern evolution process after the IP_3 concentration is changed to 0.3196 μM. The growth of the homogeneous area with a high Ca^{2+} concentration can still be observed, but the reverse compression of turbulence-like to a high Ca^{2+} concentration pattern does not happen, and the area of a high Ca^{2+} concentration pattern is fixed at about 85 percents of the whole medium. When the changed IP_3 concentration exceeds 0.3364 μM, the high Ca^{2+} concentration pattern can occupy the whole medium (see Fig.8).

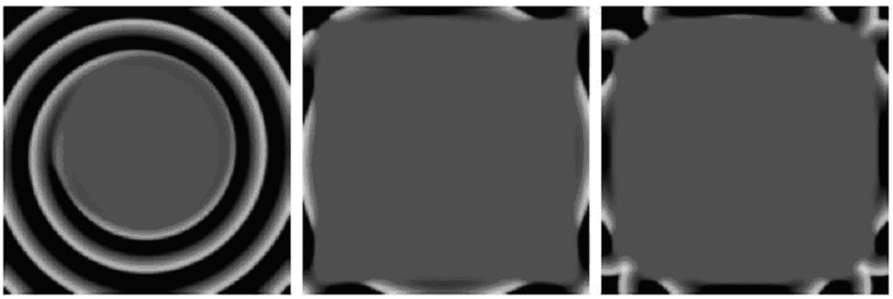


Fig.7. Time sequence illustrating the dynamics of spiral evolution when the IP_3 concentration is changed to 0.3196 μM. From left to right, t = 100, 200, and 1000 s.

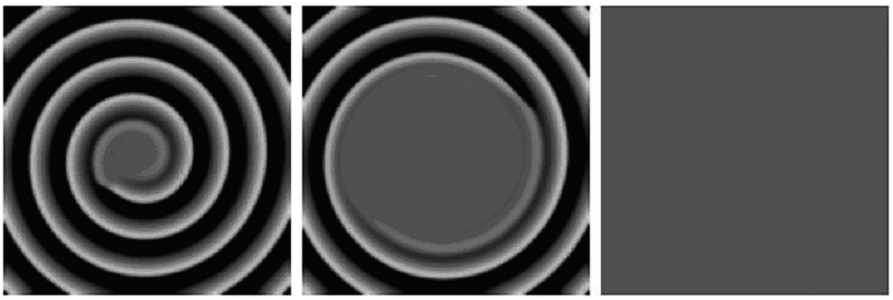


Fig.8. Time sequence illustrating the dynamics of spiral evolution when the IP_3 concentration is changed to 0.3474 μM. From left to right, t = 20, 50, and 150 s.

Comparing the pattern evolutions in Figs.5–8, the instability of spiral can be seen to be in competition between two patterns (spiral pattern and homogeneous state with a high Ca^{2+} concentration). In Fig.9, the approximate values of the homogeneous area are plotted against time for different changed IP_3 concentrations. When I = 0.3158 μM, although the homogeneous area emerges, it fails to dominate the pattern. At the critical value of I = 0.3196 μM, the homogeneous area exhibits an oscillatory behaviour. A higher IP_3 concentration (I = 0.3329 μM) can make the homogeneous area dominated and even it can occupy the whole medium when I = 0.3474 μM.

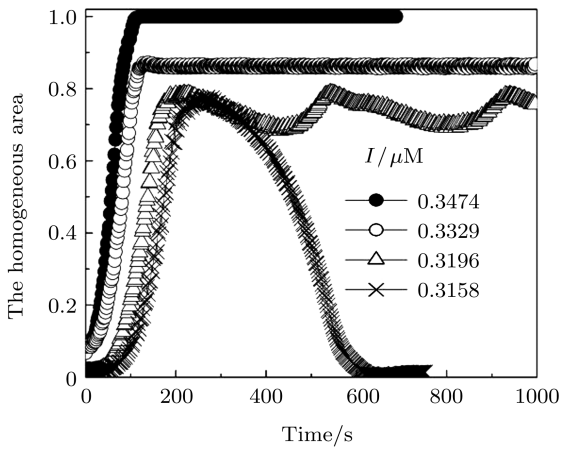


Fig.9. Time evolution of the homogeneous area (in unit of the area of the whole medium) after the IP_3 concentration is increased to different values.

In biology, the increasing of IP_3 concentration can enhance the probability for Ca^{2+} to be released through ion channels, and the medium is easier to be excited. But when IP_3 concentration is too high ($> 0.3133\,\mu$M), the medium will be easily excited and stay in a state with a high Ca^{2+} concentration. A high enough IP_3 concentration ($> 0.3364\,\mu$M) can bring the whole medium to the homogeneous state with a high Ca^{2+} concentration.

The pattern evolution for increased IP_3 concentration ($> 0.27\,\mu$M) can also be understood in terms of the local dynamics of this model. In Fig.1, with the increase of IP_3 concentration, the highest fixed point becomes closer to the uppermost point of c nullcline, so the corresponding stationary state becomes stable with the increase of IP_3 concentration. On the contrary, the stable stationary state with the lowest Ca^{2+} concentration gradually disappears with the increasing of IP_3 concentration. For example, the nullclines of the model for $I = 0.3474\,\mu$M are plotted in Fig.10, we can see that the lower stationary state corresponding to Fig.1 has disappeared and the highest stationary state becomes stable. The Ca^{2+} concentration in the homogeneous area grown from spiral centre equals that of the highest stable states obtained from the nullclines for different IP_3 concentrations. Thus the competition between two kinds of patterns in Figs.5–8 is, in fact, the competition of two stationary states, separately with the lowest and the highest Ca^{2+} concentrations. At lower IP_3 concentrations, the former pattern or stationary state dominates the medium, the latter pattern or stationary state will be the dominant one with a higher IP_3 concentration. In this context, the instability of spiral pattern is ascribed to the emergence of another stable state with a higher Ca^{2+} concentration, which has been discussed by Falcke *et al* in Ref.[17], where the emergence of new stable state is attributed to the change of parameter $V_{\max}^1$.

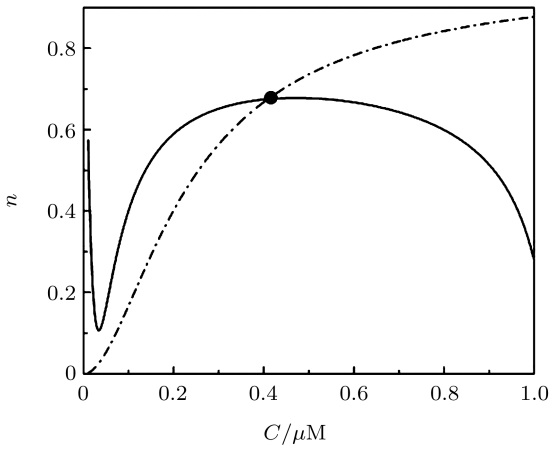


Fig.10. Nullclines of the Tang–Othmer model with $I = 0.3474\,\mu$M.

In summary, using a spatially-extended Tang–Othmer Ca^{2+} model, the effect of IP_3 concentration on Ca^{2+} pattern formation is studied numerically. When the IP_3 concentration is changed from $0.27\,\mu$M, a physiologically reasonable values, to different values, the spiral pattern evolution processes are recorded. When the IP_3 concentration is changed to a value less than $0.27\,\mu$M, the central area of spiral gradually disappears, then the open end of remaining part will curl up into a new spiral tip which is far away from the central area (see Fig.3). With the decrease of the changed IP_3 concentration, the new spiral tip becomes closer to the edge of the medium and disappears finally (see Fig.4).

This instability of spiral is ascribed to a reduction in excitability by decreasing the IP_3 concentration. On the other hand, when the IP_3 concentration is changed to a value larger than $0.27\,\mu$M, a homogeneous area with a high Ca^{2+} concentration emerges and competes with the spiral. With the increase of the changed IP_3 concentration, the homogeneous area gradually becomes a dominating pattern (see Figs.5–8). This competition can be explained through the stability of the stationary states of the system.

It is obviously that the spiral pattern evolutions are very sensitive to the IP_3 concentration in our numerical results, which maybe go beyond the controllability of experiments. But the analytical and biological explanations to the spiral instability are reasonable. Therefore, we believe that the instability mech-

anisms can be experimentally found on a larger scale of changed IP_3 concentration. On the other hand, in experiment, the most probable results are the pattern evolutions in the right bottom of Fig.4, and while from Fig.8 we can find other patterns, such as those in Fig.4, but not from Figs.5 and 7. Numerical results in these figures are helpful for us to understand the mechanism of spiral Ca^{2+} instability.

References

[1] Keener J P and Tyson J J 1986 *Physica* D **31** 307

[2] Jakubith S, Rotermund H H, Engel W, Oertzen A V and Ertl G 1990 *Phys. Rev. Lett.* **65** 3013
Rotermund H H, Jakubith S, Oertzen A V and Ertl G 1991 *Phys. Rev. Lett.* **66** 3083
Krischer K, Eiswirth M and Ertl G 1992 *J. Chem. Phys.* **96** 9161

[3] Loomis W F 1979 *Dev. Biol.* **70** 1
Tyson J J, Alexander K A, Manoranjan V S and Murray J D 1989 *Physica* D **34** 193

[4] Davidenko J M, Pertsov A M, Salomonsz K, Baxter W T and Jalife J 1991 *Nature* **355** 349

[5] Cornell-Bell A H, Finkbeiner S M, Cooper M S and Smith S J 1990 *Science* **47** 470

[6] Golovina V A and Blaustein M P 1997 *Science* **275** 1643

[7] De Koninck P and Schulman H 1998 *Science* **279** 227

[8] Dolmetsch R E, Xu K and Lewis R S 1998 *Nature* **392** 933

[9] Allen G J, Chu S P, Schumacher K, Shimazaki C T, Vafeados D, Kemper A, Hawke S D, Tallman G, Tsien R Y, Harper J F, Chory J and Schroeder J I 2000 *Science* **289** 2338

[10] Ridgway E B, Gilkey J C and Ja_e L F 1977 *Proc. Natl. Acad. Sci.* USA **74** 623

[11] Fontanilla R A and Nuccitelli R 1998 *Biophys. J.* **75** 2079
Lechleiter J, Girard S, Peralta E and Clapham D 1991 *Science* **252** 123

[12] Lechleiter J D, Johnb L M and Camacho P 1998 *Biophys. Chem.* **72** 123

[13] Falcke M, Hudson J L, Camacho P and Lechleiter J D 1999 *Biophys. J.* **77** 37

[14] Zhang H, Hu B, Hu G and Xiao J 2003 *J. Chem. Phys.* **119** 4468
Chen J X, Zhang H and Li Y Q 2006 *J. Chem. Phys.* **124** 014505

[15] Yang H J, Yang J Z and Hu G 2007 *Chin. Phys. Lett.* **24** 2752
Ma J, Ying H P, Pan G W and Pu Z S 2005 *Chin. Phys. Lett.* **22** 2752
Ma J, Chen Y and Jin W Y 2007 *Commun. Theor. Phys.* **47** 675
Ma J, Wang C N, Pu Z S and Li Y L 2006 *Commun. Theor. Phys.* **45** 1035

[16] Li B W, Sun L L, Chen B and Ying H P 2007 *Chin. Phys. Lett.* **24** 2415
Yuan G Y, Wang G R and Chen S G 2005 *Commun. Theor. Phys.* **44** 858
Wang P Y, Xie P and Yin H W 2003 *Chin. Phys.* **12** 0674
Yuan G Y, Yang S P, Wang G R and Chen S G 2008 *Chin. Phys.* B **17** 1925

[17] Falcke M, Hudson J L, Camacho P and Lechleiter J D 1999 *Biophys. J.* **77** 37
Falcke M, Or-Guil M and Bar M 2000 *Phys. Rev. Lett.* **84** 4753

[18] Sun X P, Callamaras N, Marchant J S and Parker I 1998 *J. Physiol.* **509** 67

[19] Li W H, Llopis J, Whitney M, Zlokarnik G and Tsien R Y 1998 *Nature* **392** 936

[20] Tang Y, Stephenson J L and Othmer H G 1996 *Biophys. J.* **70** 246